**International Journal of Innovative Studies in Sciences and Engineering Technology**
**ISSN 2455-4863 | Open Access | Volume 7, Issue 1, 2021**
**DOI: https://doi.org/10.20431/2455-4863.070102**

# Phoscorite From Ultrabasic Rock in Carbonatite Complex of Tiruppattur, Tamil Nadu, India

**R. Ramasamy**

*Former Deputy Director, Department of Geology and Mining, Chennai, 600 032, Tamil Nadu, India*

## ABSTRACT

Phoscorite is a rare apatite and magnetite rock with accessories of olivine and its heteromorphic variants. The close association of phoscorite and carbonatite in ultrabasic alkaline complex of Tiruppattur (N 12o15‘-12o 30’ E 78o 15’-78o25’) provides more information about volatile concentration of H2O, CO2, CH4, SO3, F, Cl, and P2O5 in mantle source and their roles on magmatic evolution of highly differentiated carbonatite complex of this area. Field evidences show that occurrence of crystallized high pressure temperature mineral (HPTM) at depth is seen in some rocks in this area. Early formed HPTM enveloped by series of layers of supercritical fluids derived by a small degree of partial melt of carbonated peridotite at mantle is stable on Earth's surface. Suddenly cracked conduit through which very rapid ascent of supercritical fluid of natrocarbonatite carrying HPTM from mantle at a speed ranging from 70 to 100 m/s within <10 hours of duration without any friction and energy loss, retains its structural stability to Earth's surface. Phoscorite and carbonatite fluids in peridotite are caused mineralization apatite and ilmenorutile in this complex.

**Keywords:** hoscorite, apatite, Magnetite, Silicate-perovskite Ultrabasic, Carbonatite complex of Tiruppattur, Tamil Nadu

## INTRODUCTION

Phoscorite is a rare apatite and magnetite rock. It occurs in carbonatite ultrabasic alkaline complex of Tiruppattur (N 12o15‘-12o 30’ E 78o 15’-78o 25’). The rock is composed of olivine and any one of its heteromorphic equivalents of diopside, acmite, hornblende, phlogopite, magnetite, calcite, feldspar and foids / quartz as accessory mineral. It provides more information about mantle source and deep-seated magmatic processes controlled by volatile concentration of H2O, CO2, CH4, SO3, F, Cl, and P2O5. These volatiles are caused formation of ultralow viscous supercritical fluid of natrocarbonatite at lower mantle where ultralow velocity seismic zone is prevailed.

## GEOLOGICAL SETTING

Carbonatite complex of Tiruppattur (N 12o15‘-12o 30’ E 78o 15’-78o25’) is comprised with 3 carbonatite units located at Sevvattur, Jogipatti and Onnakarai villages [1- 6] in association with ultrabasic rocks and alkali syenites (Fig. 1). Conesheets of carbonatite of Sevvattur is exposed (1500 x 300 m) NW at contact between ultrabasic and syenite complex in Sevvattur basin. The carbonatite varies from ferrocarbonatite, beforsite to sovite. Apart from the essential minerals [6] of calcite, dolomite, ferrocarbonate, accessory minerals of magnetite, perovskite, pyrochlore, zircon, apatite, aegirine augite, riebeckite, oligoclase and phlogopite are found as accessory minerals in the carbonatite. Concentration of pyrochlore is observed in ferrocarbonatite. Lueshite (Sodium bearing reddish brown pyrochlore) shows expansion cracks in albitite exposed at south eastern periphery of carbonatite of Sevvattur. Semitransparent and semiprecious euhedral pale reddish brown zircon is found as accessory high pressure temperature mineral (HPTM) in carbonatite of Sevvattur and metamict dark brown euhedral zircon occurs in zircon syenite exposed about 1.5 km SW of Samalpatti village. An ultrabasic rock exposes at north western boundary of the carbonatite. Phoscorite occurs as diatremes up to 7500 x 10 cm at contact of a vermiculite body on NW part of Sevvattur carbonatite. It is the largest vermiculite mine in India formed by alteration of phlogopite-oligoclase pyroxenite.

Thin veins of sovite, beforsite, ferrocarbonatite, barite and benstonite occur in ultrabasic rock exposing in Onnakarai area. The ultrabasic rock is intercalated ultramafic rock essentially composed of pyroxenite and peridotite. Phoscorites in ultrabasic rock are exposed at about 200 m SW of Onnakarai village. They occur as rootless thin diatremes of varying sizes from 100 x 5 to 5000 x 10 cm in ultrabasic rock near the village. At some places dunite and peridotite with pyroxenite dykes are seen Magnesite and kankar are released products at some places. Just south of the village barite vein 100x15cm is found.

A skarn rock (1500 x 50m) extends from Garigaipalli to Onnakarai villages [7]. Near Garigaipalli a high grade skarn trends towards NNE-SSW and steeply dipping towards WNW. An intermittent shear zone trending WNW-ESE and shift it WNW-ESE direction. There it is attained low grade metamorphism towards south forming discontinuous arc like form dipping inwards. Ultra low viscous ferrocarbonatite veins of <100x5 cm carrying euhedral magnetite (< 5mm) are seen along some shear zones trending in WNW-ESE direction. Monazite bearing pegmatite and galena bearing fine-grained albitite [8] occur at contact between syenite and skarn in SW part. Ultrabasic nodules of varying sizes between 1 and 50 cm dimensions [7] are seen in the skarn. The nodule occasionally contains native Cu and Ag in addition to chalcopyrite, covellite, cuprite, malachite and azurite, sphalerite, pyrite, phyrrhotite and galena [8]. The skarn and nodules are composed with tightly folded veins with alternate miniature swelled micro-basins and tightly compressed micro-domes. A single nodule comprises single basin and a dome. Wollastonite, diopside, garnet scapolite and calcite are seen as major minerals. Epidote and vesuvenite crystallize along some weak planes of the rock. Ultrapotassic syenite of microcline-melanite syenite [9] and garnet-syenite, anorthoclase-riebeckite potassic syenite occur as major rock types in Jogipatti basin.

NE-SW trending elongated small rings of carbonatite veins are seen in Jogipatti village along fold axial planes of the structural basin. The basin is located hardly 5 km SW of Sevvattur basin (Fig. 1). Both basins occur in NE-SW direction trending along Alangayam rift zone which is further extending over Amirthi fault near Vellore and further NE to Bay of Bengal, on SW it extends over 400 km into Arabian Sea [10]. The present width of the rift zone exceeds over 50 km at some places. Faulted Jogipatti basin including carbonatites and potassic syenites has uplifted 1600 m from NNE-SSW to NE-SW relative to Sevvattur basin which is sequentially filled with sodium syenites. Along a fault zone lying between the basins Jogipatti basin is rotated to 16o NE-SW [2, 5] Younger co-magmatic sequences are progressively differentiated and are emplaced in sequences in SW parts of these structural basins (2). There exists magmatic continuum between older sodium and younger potassium rich syenites [2, 5].

## METHODOLOGY

The phoscorite was analyzed using High Resolution Scanning Electron Microscope attached with EDAX probe in the Laboratory, Department of Metallurgical and Material Science, Indian Institute of Technology, Chennai. The elemental analyses were recalculated and Rittmann's normative proportions were calculated [11]. Iron ores were subjected X-ray powder diffractions analyses with Fe Ka radiations were made in the crystallography Department of Geology Faculty of Moscow State University, Russia. The minerals had mixed proportions of iron ores and they were difficult to distinguish individual components and indexing their faces. However, all the peaks and their intensities are given for future references (Table 1). Characteristic peaks of magnetite of were listed (Table 2) for correlation.

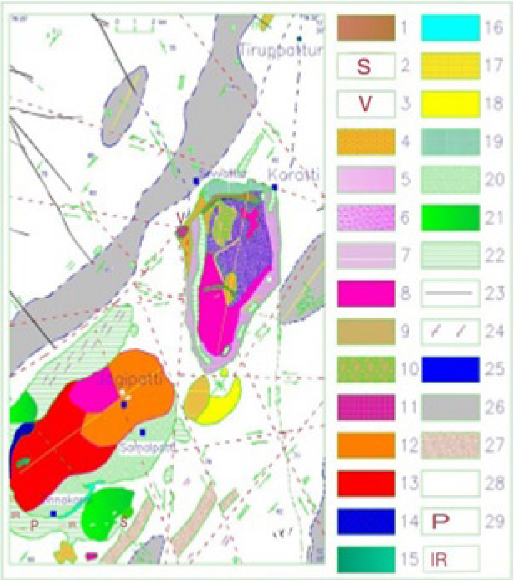

**Fig1.** Simplified Geological map of carbonatite complex of Tiruppattur, Tamil Nadu, India

1 Carbonatite, 2 S Shonkinite 3 V Vogesite 4 Oligoclasite 5 Hornblende syenite 6 Hornblende porphyric syenite 7 Augite syenite 8 Porphyritic augite syenite 9 Foliated syenite 10 Foliated porphyritic syenite 11 Hornblende biotite syenite 12 Riebeckite syenite 13 Garnetiferous syenite 14 Microcline melanite syenite 15 Wollastonite syenite 16. Skarn 17 Granite 18 Granodiorite 19 Biotite oligoclase pyroxenite 20 Biotite pyroxenite 21 Ultrabasics 22 Ultramafics 23 Dolerites 24 Pegmatite / aplite 25 Albitite 26 Charnockite 27 Pyroxene granulite 28 Granite gneisses P Phoscorite IR Ilmenorutile

## PETROGRAHY AND PETROCHEMISTRY

On hand examination in the field, phoscorite appears to be a feldspar-magnetite rock and it is subjected to wet-gravimetric analysis. Before wet-gravimetric analysis, spectroscopic analyse shows a high concentration of P, Fe, Ti, Y, Nb and Zr reveals that the rock is essentially composed of apatite nioborutile (ilmenorutile), zircon and magnetite Under polarizing microscope apatite exhibits euhedral form with strong relief and first order grey interference colour and opaque iron ore. The rock is termed as phoscorite. In Sevvattur basin it is a very coarse-grained rock with inequigranular porphyritic texture. Bluish yellow green euhedral apatite up to 4x2x1 cm is seen with blades or booklets of phlogopite amidst apatite. Large grain of magnetite up to 6 cm is seen.

On the other hand, it occurs 700 m NE of Mottusulakkarai village and 200 m SW of Onnakarai village and carries reddish brown massive apatite up to 2x0.5 cm and magnetite up to 1.5 x 0.5 cm with coarse-grained inequigranular porphyritic texture. Scanning electron microscope images show particle size of (Fig. 2) larger plates of euhedral prism and pyramid shaped apatite up to 180x60x3 μm form with length, breadth and thickness. Tabular apatite grains overlap one over the other as platelets. Apatite has transverse irregular gas cavities (Fig:-2). A globular gas cavity of 150 μm is filled with smaller but inequigranular prisms of apatite and other minerals. The gas cavities are aligned along peripheral portions and at the central portion of globular cavity. Around periphery of some irregular cavities, rims of very fine-grained minerals are developed. Cavities are represented as fluid phases. Particle size of magnetite 250x150x30μm is found. Edges of magnetite are very sharp and steep. Phlogopite flake of 200x5x1 μm is seen.

XRD analyses of apatite (Cu Ka) and magnetite (Fe Ka) from Sevvattur, Jogipatti and Onnakarai are also listed in the Table 1. The 2Theta values for iron ores on Fe Ka radiations show characteristic peaks for magnetite on faces of Miller's indices. The slight deviations from normal peaks might have been due to solid solution and entry of other elements, distortion of crystal faces or interference of mixed phases formed at ambient temperature and pressure conditions. Table-2 such variations are seen in magnetite. Magnetite (mt1) shows very low values of 2Theta for Fe Ka radiations might have been representing entry of silica perovskite molecules in magnetite in Table 1.

**Table1.** X-ray powder diffraction data for apatite Cu Ka and magnetite for Fe Ka radiation .

| Mt | 456 | Sevvatur | | Ap-rock | 450 | Onnakarai | | Mt | 1 | Sevvatur | | Mt | 2 | Sevvatur | |
|---|---|---|---|---|---|---|---|---|---|---|---|---|---|---|---|
| 2θFeKa | I/Io | CuKa A | FeKa A | 2θ CuKa | I/Io | A CuKa | A FeKa | 2θFeKa | I/Io | CuKa A | FeKa A | 2θFeKa | I/Io | CuKa A | FeKa A |
| 38.22 | 41.20 | 2.3547 | 3.00 | 11.10 | 9 | 7.8711 | 10.00 | 6.90 | 4 | 12.9989 | 16.30 | 22.98 | 5 | 3.8701 | 4.90 |
| 40.60 | 25.00 | 2.2220 | 2.80 | 22.45 | 3 | 3.9603 | 5.00 | 7.40 | 4 | 11.9463 | 15.00 | 38.12 | 32 | 2.3607 | 3.00 |
| 41.44 | 14.70 | 2.1789 | 2.70 | 26.40 | 32 | 3.3761 | 4.20 | 23.36 | 7 | 3.8080 | 4.80 | 45.12 | 100 | 2.0094 | 2.50 |
| 42.10 | 23.50 | 2.1462 | 2.70 | 27.95 | 13 | 3.1923 | 4.00 | 30.68 | 6 | 2.8557 | 3.60 | 47.24 | 6 | 1.9241 | 2.40 |
| 45.20 | 100.00 | 2.0060 | 2.50 | 28.76 | 11 | 3.1041 | 3.90 | 38.38 | 37 | 2.3465 | 2.90 | 55.10 | 54 | 1.6669 | 2.10 |
| 53.80 | 16.20 | 1.7874 | 1.80 | 29.40 | 25 | 3.0380 | 3.80 | 42.36 | 34 | 2.1337 | 2.70 | 69.12 | 16 | 1.3590 | 1.70 |
| 66.84 | 19.10 | 1.3036 | 1.70 | 32.40 | 100 | 2.7632 | 3.50 | 45.40 | 100 | 1.9577 | 2.50 | 72.88 | 61 | 1.3000 | 1.60 |
| 74.00 | 27.90 | 1.2909 | 1.60 | 32.70 | 57 | 2.7388 | 3.40 | 47.32 | 7 | 1.9210 | 2.40 | 81.72 | 52 | 1.2000 | 1.50 |
| 78.46 | 8.80 | 1.2189 | 1.60 | 33.53 | 50 | 2.6727 | 3.40 | 52.40 | 9 | 1.7461 | 2.20 | | | | |
| 80.26 | 11.80 | 1.1961 | 1.60 | 34.58 | 19 | 2.5866 | 3.20 | 55.40 | 63 | 1.6582 | 2.10 | | | | |
| 81.78 | 51.50 | 1.1776 | 1.50 | 35.80 | 6 | 2.5082 | 3.20 | 63.64 | 12 | 1.4621 | 1.80 | | | | |
| 84.10 | 10.30 | 1.1510 | 1.40 | 39.78 | 8 | 2.2660 | 2.80 | 69.18 | 17 | 1.3580 | 1.70 | | | | |
| | | | | 40.52 | 21 | 2.2263 | 2.80 | 70.10 | 17 | 1.3000 | 1.70 | | | | |
| | | | | 42.58 | 5 | 2.1182 | 2.70 | 74.20 | 70 | 1.3000 | 1.60 | | | | |
| | | | | 44.40 | 4 | 2.0403 | 2.60 | 81.90 | 70 | 1.2000 | 1.50 | | | | |
| | | | | 47.30 | 23 | 1.9218 | 2.40 | | | | | | | | |
| | | | | 48.76 | 11 | 1.8676 | 2.30 | | | | | | | | |
| | | | | 49.30 | 11 | 1.8483 | 2.30 | | | | | | | | |
| | | | | 50.08 | 31 | 1.8214 | 2.30 | | | | | | | | |
| | | | | 51.10 | 13 | 1.7874 | 2.20 | | | | | | | | |
| | | | | 51.98 | 11 | 1.7611 | 2.20 | | | | | | | | |
| | | | | 52.88 | 10 | 1.7366 | 2.20 | | | | | | | | |
| | | | | 53.52 | 21 | 1.7122 | 2.20 | | | | | | | | |
| | | | | 54.40 | 4 | 1.6866 | 2.10 | | | | | | | | |
| | | | | 56.58 | 8 | 1.6265 | 2.00 | | | | | | | | |
| | | | | 60.40 | 5 | 1.5326 | 1.90 | | | | | | | | |
| | | | | 62.08 | 8 | 1.4951 | 1.90 | | | | | | | | |
| | | | | 63.60 | 13 | 1.4630 | 1.80 | | | | | | | | |
| | | | | 64.56 | 11 | 1.4435 | 1.80 | | | | | | | | |
| | | | | 65.84 | 8 | 1.4223 | 1.80 | | | | | | | | |
| | | | | 70.40 | 5 | 1.3000 | 1.70 | | | | | | | | |

| Mt | 3 | Sevvattur | | Mt | 4 | Sevvattur | | Mt | 5 | Sevvattur | | M1 | 6 | Sevvattur | |
|---|---|---|---|---|---|---|---|---|---|---|---|---|---|---|---|
| 2θFeKα | I/Io | CuKα A | FeKα A | 2θFeKα | I/Io | CuKα A | FeKα A | 2θFeKα | I/Io | CuKα A | FeKα A | 2θFeKα | I/Io | CuKα A | FeKα A |
| 23.10 | 8 | 3.8503 | 4.80 | 17.90 | 18 | 4.9554 | 6.20 | 38.24 | 21 | 2.7760 | 2.9669 | 38.28 | 24 | 2.3523 | 2.9559 |
| 38.16 | 25 | 3.3584 | 3.00 | 23.30 | 4 | 3.8177 | 4.80 | 41.44 | 25 | 2.1790 | 2.7378 | 44.70 | 25 | 2.0273 | 2.5471 |
| 41.46 | 12 | 2.7780 | 2.70 | 30.40 | 4 | 2.9403 | 3.70 | 42.22 | 39 | 2.1406 | 2.6892 | 45.22 | 100 | 2.0051 | 2.5192 |
| 42.20 | 5 | 2.1415 | 2.70 | 38.32 | 20 | 2.3469 | 3.00 | 45.20 | 100 | 2.0060 | 2.5206 | 55.18 | 26 | 1.6645 | 2.0912 |
| 45.17 | 100 | 2.0073 | 2.60 | 41.44 | 14 | 2.1790 | 2.70 | 52.36 | 14 | 1.7418 | 2.1855 | 69.00 | 13 | 1.3610 | 1.7102 |
| 47.32 | 5 | 1.9210 | 2.40 | 42.32 | 13 | 2.1357 | 2.70 | 55.34 | 18 | 1.6600 | 2.0894 | 73.96 | 43 | 1.2815 | 1.6107 |
| 51.48 | 3 | 1.7751 | 2.20 | 45.24 | 100 | 2.0044 | 2.50 | 63.64 | 19 | 1.4624 | 1.8373 | 81.78 | 54 | 1.1776 | 1.4800 |
| 55.16 | 33 | 1.6651 | 2.10 | 47.36 | 4 | 1.9195 | 2.40 | 68.64 | 10 | 1.3655 | 1.7184 | 94.10 | 16 | 1.0532 | 1.3233 |
| 69.18 | 11 | 1.3579 | 1.70 | 52.24 | 5 | 1.7511 | 2.20 | 73.98 | 18 | 1.3441 | 1.6867 | | | | |
| 73.93 | 55 | 1.3000 | 1.60 | 55.16 | 31 | 1.6651 | 2.10 | 76.00 | 30 | 1.3000 | 1.6462 | | | | |
| 80.45 | 5 | 1.2000 | 1.50 | 62.90 | 6 | 1.4776 | 1.90 | 82.00 | 31 | 1.2000 | 1.4764 | | | | |
| 81.80 | 44 | 1.2000 | 1.50 | 63.55 | 4 | 1.4640 | 1.80 | 84.00 | 13 | 1.2000 | 1.4477 | | | | |
| | | | | 69.18 | 11 | 1.3580 | 1.70 | 95.44 | 11 | 1.1000 | 1.3093 | | | | |
| | | | | 70.00 | 7 | 1.3441 | 1.70 | 99.00 | 9 | 1.0000 | 1.2739 | | | | |
| | | | | 73.86 | 31 | 1.30 | 1.60 | | | | | | | | |
| | | | | 80.50 | 3 | 1.20 | 1.50 | | | | | | | | |
| | | | | 81.85 | 36 | 1.20 | 1.50 | | | | | | | | |
| | | | | 92.30 | 5 | 1.20 | 1.30 | | | | | | | | |

**Table2.** Comparative studies of 2 Theta and intensity of peaks for magnetite and apatite

| mt1 | mt2 | mt3 | mt4 | mt5 | mt6 | mt7 | mt8 | mt222 | mts498 | mtj380 | mtj381 | mto495 | mts 498 |
|---|---|---|---|---|---|---|---|---|---|---|---|---|---|
| 6.80 | | | | | | | | | | | | | |
| 7.40 | | | | | | | | | | | | | |
| 23.36 | | 17.90 | 17.90 | | | 23.02 | | | | | 28.06 | | |
| 38.36 | 38.12 | 38.32 | 38.32 | 38.24 | 38.26 | 38.54 | 38.16 | 37.64 | 38.22 | 37.44 | | 34.64 | 38.22 |
| | | 41.44 | 41.44 | | | 41.38 | 41.38 | | 41.44 | 38.10 | 41.60 | 41.20 | 41.44 |
| | | 42.32 | 42.32 | 42.22 | 44.70 | 42.24 | 42.16 | | 42.10 | 42.00 | | 44.20 | 42.10 |
| 46.40 | 46.12 | 46.24 | 46.24 | 46.20 | 45.22 | 46.18 | 46.16 | 44.64 | 46.20 | 46.18 | 46.20 | 46.80 | 45.20 |
| 55.40 | 55.10 | 55.16 | 55.16 | 55.34 | 55.18 | 55.14 | 55.22 | 54.80 | 68.84 | 55.12 | 55.22 | 58.00 | 68.84 |
| 74.20 | 72.88 | 73.86 | 73.86 | 72.40 | 73.96 | 73.92 | 73.92 | 73.44 | 74.00 | 73.94 | 74.02 | 73.10 | 74.00 |
| 81.90 | 81.72 | 81.85 | 81.85 | 84.40 | 81.78 | 81.80 | 81.80 | 81.42 | 81.78 | 81.80 | 81.84 | | 81.78 |
| | | | | | | 98.90 | | | 84.10 | 94.22 | 94.26 | 90.76 | 84.10 |

Inner core of ultrabasic nodule free from any feldsic constituents in skarn rock is chemically analyzed. It is composed of SiO2 45.92, Al2O3 6.12, Fe2O3 5.52, FeO 5.33, MnO 0.18, MgO 9.60, CaO 22.46, Na2O 1.08, K2O 0.16, TiO2 1.26, P2O5 0.19, CO2 1.02 and H2O 0.50 wt% and has high content of MgO, CaO and SiO2. The characteristic trace elements are Ba 2000, Zr 10, V 300, Cu 100, Zn 300, Cr 100, Ni 60, Co 30, and Pb 8 ppm. The normative proportion of the rock is cc 2.63, ap 0.46, il 1.63, mt 2.06, ol 16.64, hy 15.78, wo 37.85 and lab 22.76%. Microscopic studies reveal that presence of wollastonite, (Fig. 3) grossularite-andradite garnet and scapolite. It exhibits hypidiomorphic granular texture. Aplite and pegmatite of wollastonite-garnet sovite, wollastonite garnet syenite and melanite microcline ultrapotassic syenite have genetic link with skarn [7, 8]. Ferric iron are seen (Fig. 3) as opaque dusts [12, 15] in potassic feldspars in ultrapotassic melanite syenite, shonkinite and in ultrabasic rocks. Scapolite – arfvedsonite syenites are seen around carbonatites of Jogipatti.

Chemical analyses of magnetite from Sevvattur show progressively increasing silica content from 0.48 to 62.14%. The degree of oxidation (Fe3/Fe3+Fe2+Mn) of magnetites varies between O.39 and 0.96. Maghemite phase is enriched with higher oxidation degree. This phase is found in all magnetite. Normative spinel is found in 498 and 13. Magnetite is polygenetic. Thin section studies reveal that it occurs as primary opaque cloudy dusts which are later oxidized and swept along grain boundaries, cleavage planes of calcite and they accumulated secondary crystals [12] in calcite of carbonatite. Scapolite – arfvedsonite syenites are seen around carbonatites of Jogipatti.

Some magnetite [13] have enriched with Ca ions on the basis of 32 (O, OH, F). Ca is present in 13 up to 3.205 ions (Table 4) indicating entry of perovskite. Si content of magnetite steadily increases from 498Si 0.141, 13Si 5.459, 21Si 8.717 and 47Si 11.840. Generally under alkaline condition porous silica is introduced to overall surface area in magnetite from 8.2 to 13.2 nm [14]. At HPT condition incorporation of Si in magnetite transits it into silicate perovskite under ambient HPT state.

Ca rich pyroxene [15] and Ti rich garnet show magmatic courses of differentiation [16] in this complex. Sr replaces Ca in apatite [13] on the basis of 26 (O, OH, H) Table 5. Fluorite and periclase enter in apatite. Si, Al and Mg (Table 6) substitute into apatite structure. Olivine content varies between 7 and 31%. Flour-apatite varies up to 90-97; fluorite up to 8; Ca bearing olivine 1 and portlandite has 5% (Table 5). Table 6 shows that 46-66% of apatite. It is enriched with Ca-olivine 23 portlandite 23, bytownite(ab24 - an76), 13% and nepheline 4 with or without kalsilite 1% are present to meet silica deficiency. Highly transparent and pale yellowish green phlogopite is found from phoscorite in Sevvattur. The ratio of Mg/(Mg + Fe) is 0.678 (Table 4) indicates it is phlogopite. It shows III or IV order interference colour. Structural formula on the basis of 22 (O, OH, F), the phlogopite has lost considerable amount of Si, Al, Mg, K, and $H_2O^+$. Ca exist 0.483 apfu which is higher than normal phlogopite (Table 4). Fluorine occurs in apatite up to 0.823 on the basis of 26 (O, OH, F) ions (Table 5). Normative fluorite reaches to 7 %. Pure apatite of Sevvattur is silica under saturated and has minute opaque inclusions of periclase up to 5%. $SiO_2$ varies up to 16.80% (Table 6) and it has normative nepheline 4 with or without kalsilite 1%. Apatite is present up to 55%. Locally, the ratio of apatite and iron ore is 79 : 21. There exists close relationship [17] between increase of apatite saturation and decreasing of silica content in mafic-alkali magma.

EDAX analyses (Table 7) of phoscorite of Onnakarai area show enrichment of FeO, $TiO_2$, $Nb_2O_5$, $ZrO_2$ and $REE_2O_3$. In Onnakarai the host rock of phoscorite is peridotite which is composed of Ca- olivine (Table 3) 45, clinopyroxene 32, calcic plagioclase 13 and apatite 6%. Phoscorite is composed of apatite 19-74, calcite 7, anhydrite 3 and iron ore 25% (Table 3 and 7). Olivine breaks down into pyroxene (451) and quartz at ambient temperature and pressure condition (Table 3). Table 7 shows that phoscorite is composed of apatite, ilmenorutile, perovskite as essential minerals [18]. The enrichments of $TiO_2$, $Nb_2O_5$, $SiO_2$, $Y_2O_3$ and other REE oxides are caused by presence of silicate perovskite. It is composed of $SiO_2$ 2.0, $Al_2O_3$ 1.5, FeO 26.0, MnO 2.0, MgO 0.5, CaO 15.0, $Na_2O$ O.5, $K_2O$ 0.5, $TiO_2$ 25.0, $P_2O_5$ 13.0, F 0.5, $SO_3$ 1.5, $Y_2O_3$ 7.0, $ZrO_2$ 4.0 and $Nb_2O_5$ 24.0%.

Phoscorites and carbonatites appear to be formed at end stages [27] of magmatic differentiation and fractionation with intermittent liquid immiscibility [1-6, 8, 15, 16, 18 -26]. These nil silicate rocks superimpose one over the other in the field of Si-P-(Fe+Mn) for phoscorite (Fig.4). Large and dense ilmenorutile up to 15x10x8 cm are commonly found as floats around Onnakarai village.

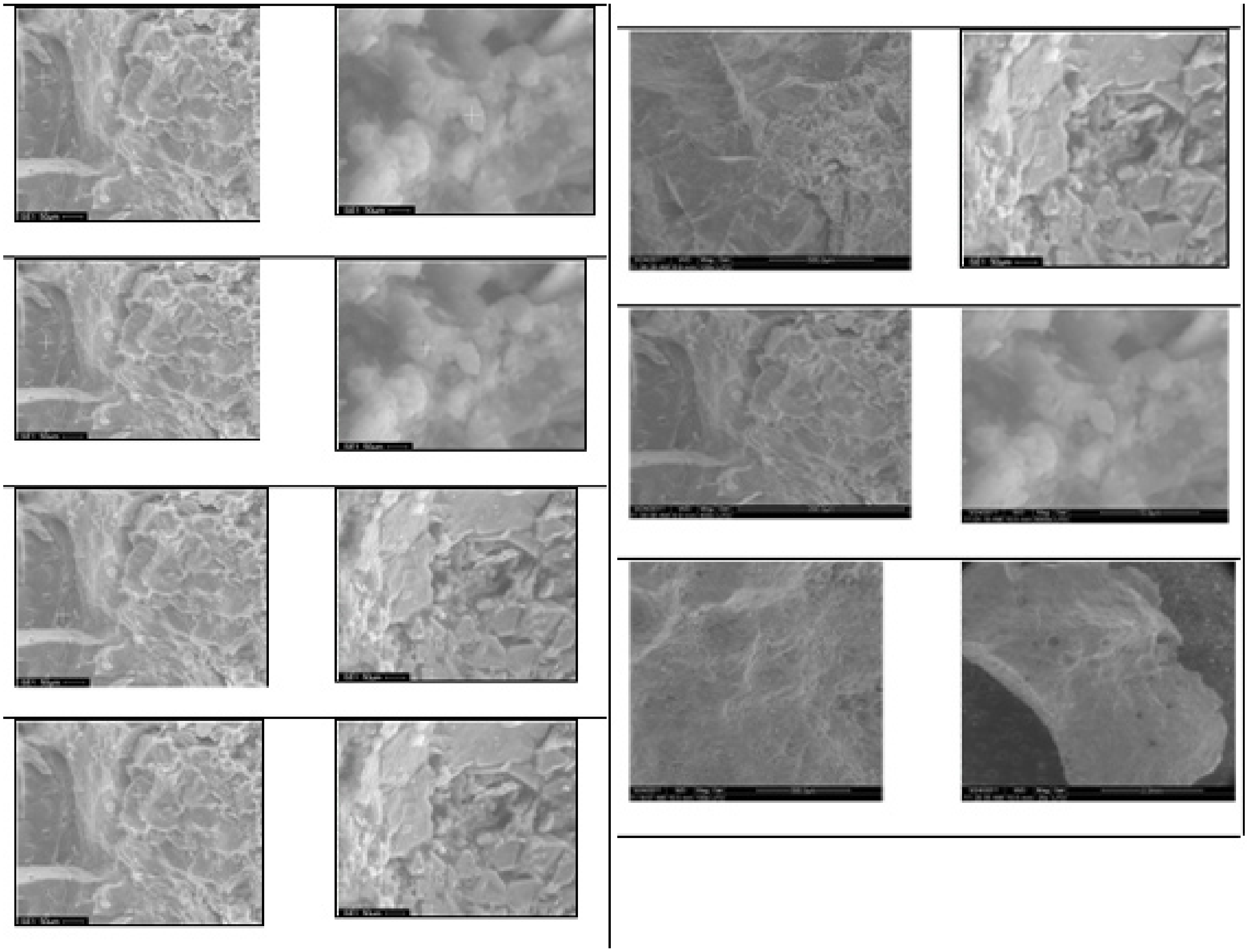

**Fig2.** The EDAX images of phoscorite show essential minerals of apatite and iron ore.

**Table3.** Wet-gravimetric analyses of magnetite (498, 13, 21, 47) from phoscorite from Sevvattur and phoscorite 451, apatite 450 and a host rock of peridotite 40 from Onnakarai are given below:

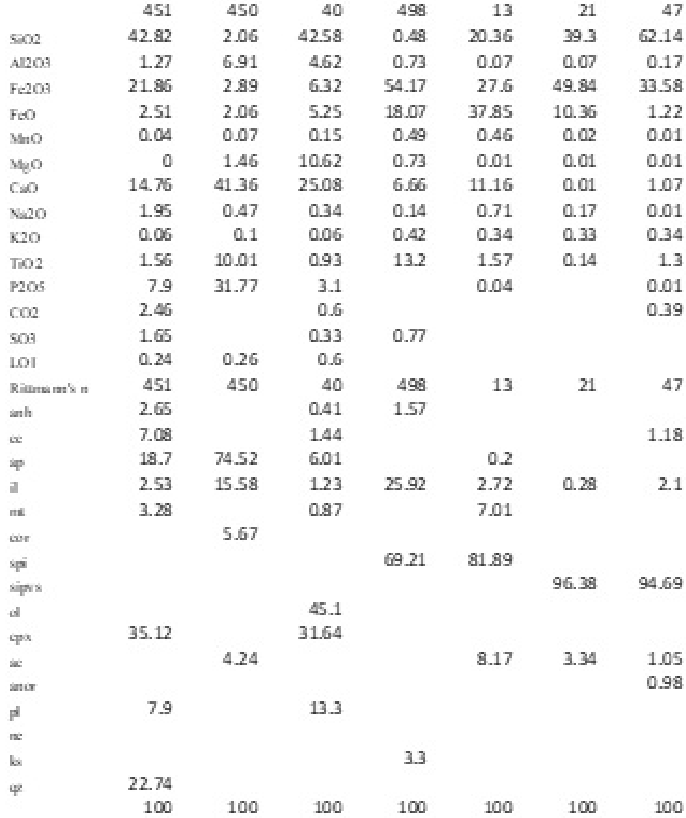

| | 451 | 450 | 40 | 498 | 13 | 21 | 47 |
|---|---|---|---|---|---|---|---|
| SiO2 | 42.82 | 2.06 | 42.58 | 0.48 | 20.36 | 39.3 | 62.14 |
| Al2O3 | 1.27 | 6.91 | 4.62 | 0.73 | 0.07 | 0.07 | 0.17 |
| Fe2O3 | 21.86 | 2.89 | 6.32 | 54.17 | 27.6 | 49.84 | 33.58 |
| FeO | 2.51 | 2.06 | 5.25 | 18.07 | 37.85 | 10.36 | 1.22 |
| MnO | 0.04 | 0.07 | 0.15 | 0.49 | 0.46 | 0.02 | 0.01 |
| MgO | 0 | 1.46 | 10.62 | 0.73 | 0.01 | 0.01 | 0.01 |
| CaO | 14.76 | 41.36 | 25.08 | 6.66 | 11.16 | 0.01 | 1.07 |
| Na2O | 1.95 | 0.47 | 0.34 | 0.14 | 0.71 | 0.17 | 0.01 |
| K2O | 0.06 | 0.1 | 0.06 | 0.42 | 0.34 | 0.33 | 0.34 |
| TiO2 | 1.56 | 10.01 | 0.93 | 13.2 | 1.57 | 0.14 | 1.3 |
| P2O5 | 7.9 | 31.77 | 3.1 | | 0.04 | | 0.01 |
| CO2 | 2.46 | | 0.6 | | | | 0.39 |
| SO3 | 1.65 | | 0.33 | 0.77 | | | |
| LOI | 0.24 | 0.26 | 0.6 | | | | |
| Rittmann's n | 451 | 450 | 40 | 498 | 13 | 21 | 47 |
| anh | 2.65 | | 0.41 | 1.57 | | | |
| cc | 7.08 | | 1.44 | | | | 1.18 |
| ap | 18.7 | 74.52 | 6.01 | | 0.2 | | |
| il | 2.53 | 15.58 | 1.23 | 25.92 | 2.72 | 0.28 | 2.1 |
| mt | 3.28 | | 0.87 | | 7.01 | | |
| cor | | 5.67 | | | | | |
| spi | | | | 69.21 | 81.89 | | |
| sipvs | | | | | | 96.38 | 94.69 |
| ol | | | 45.1 | | | | |
| cpx | 35.12 | | 31.64 | | | | |
| ac | | 4.24 | | | 8.17 | 3.34 | 1.05 |
| anor | | | | | | | 0.98 |
| pl | 7.9 | | 13.3 | | | | |
| ne | | | | | | | |
| ks | | | | 3.3 | | | |
| qz | 22.74 | | | | | | |
| | 100 | 100 | 100 | 100 | 100 | 100 | 100 |

**Table4.** Analysis of Magnetite and their structural formula (Magnetite 32 (O, OH, F), apatite 26 (O, OH, F) Phlogopite 22 (O, OH F)

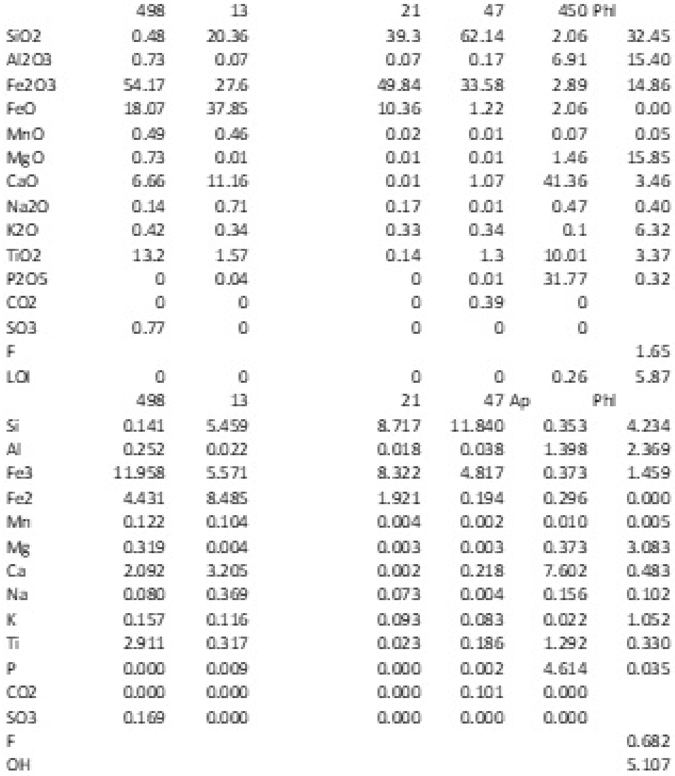

| | 498 | 13 | 21 | 47 | 450 | Phl |
|---|---|---|---|---|---|---|
| SiO2 | 0.48 | 20.36 | 39.3 | 62.14 | 2.06 | 32.45 |
| Al2O3 | 0.73 | 0.07 | 0.07 | 0.17 | 6.91 | 15.40 |
| Fe2O3 | 54.17 | 27.6 | 49.84 | 33.58 | 2.89 | 14.86 |
| FeO | 18.07 | 37.85 | 10.36 | 1.22 | 2.06 | 0.00 |
| MnO | 0.49 | 0.46 | 0.02 | 0.01 | 0.07 | 0.05 |
| MgO | 0.73 | 0.01 | 0.01 | 0.01 | 1.46 | 15.85 |
| CaO | 6.66 | 11.16 | 0.01 | 1.07 | 41.36 | 3.46 |
| Na2O | 0.14 | 0.71 | 0.17 | 0.01 | 0.47 | 0.40 |
| K2O | 0.42 | 0.34 | 0.33 | 0.34 | 0.1 | 6.32 |
| TiO2 | 13.2 | 1.57 | 0.14 | 1.3 | 10.01 | 3.37 |
| P2O5 | 0 | 0.04 | 0 | 0.01 | 31.77 | 0.32 |
| CO2 | 0 | 0 | 0 | 0.39 | 0 | |
| SO3 | 0.77 | 0 | 0 | 0 | 0 | |
| F | | | | | | 1.65 |
| LOI | 0 | 0 | 0 | 0 | 0.26 | 5.87 |
| | 498 | 13 | 21 | 47 Ap | Phl | |
| Si | 0.141 | 5.459 | 8.717 | 11.840 | 0.353 | 4.234 |
| Al | 0.252 | 0.022 | 0.018 | 0.038 | 1.398 | 2.369 |
| Fe3 | 11.958 | 5.571 | 8.322 | 4.817 | 0.373 | 1.459 |
| Fe2 | 4.431 | 8.485 | 1.921 | 0.194 | 0.296 | 0.000 |
| Mn | 0.122 | 0.104 | 0.004 | 0.002 | 0.010 | 0.005 |
| Mg | 0.319 | 0.004 | 0.003 | 0.003 | 0.373 | 3.083 |
| Ca | 2.092 | 3.205 | 0.002 | 0.218 | 7.602 | 0.483 |
| Na | 0.080 | 0.369 | 0.073 | 0.004 | 0.156 | 0.102 |
| K | 0.157 | 0.116 | 0.093 | 0.083 | 0.022 | 1.052 |
| Ti | 2.911 | 0.317 | 0.023 | 0.186 | 1.292 | 0.330 |
| P | 0.000 | 0.009 | 0.000 | 0.002 | 4.614 | 0.035 |
| CO2 | 0.000 | 0.000 | 0.000 | 0.101 | 0.000 | |
| SO3 | 0.169 | 0.000 | 0.000 | 0.000 | 0.000 | |
| F | | | | | | 0.682 |
| OH | | | | | | 5.107 |

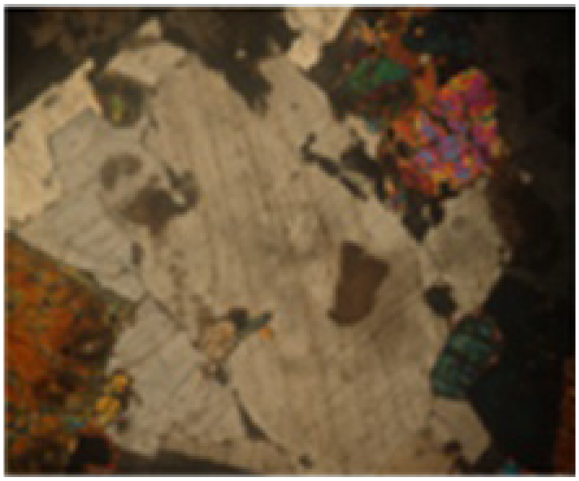

**Fig3.** 1 Opaque fine dusts in potash feldspars in panidiomorphic shonkinite 2 Lueshite with expansion cracks in albitite 3 Garnet bearing pyroxenite 4 Garnet syenite  5 Secondary magnetite in sovite 6 Skarn shows garnet, wollastonite, diopside scapolite and plagioclase.

It is essentially composed apatite 40% and ilmenorutile 60%.The distribution of Si, P and Fe + Mn in [27] an equilateral triangle in Fig. 4 shows that phoscorite is differentiated from carbonatite into apatite – magnetite end. Similar feature is seen in Fig. 5.  This may be further illustrated in Fig. 6.  Fig. 6 classifies without adding heteromorphic equivalents to olivine. Therefore fields of olivine shrinks hence, olivine rich or olivine poor phoscorites are absent [27]. A linear variation (Fig. 7) is present between K2O vs CaO/ Al2O3. Most rocks the ratios of CaO/Al2O3 are limited to <10 (Fig. 7) indicating [27] low to medium degree of partial melting of carbonated peridotite at depth. SiO2 vs MgO shows a linear positive variation [27] indicating differentiation. Nb2O5 + Ta2O5 vs ZrO¬2 + Hf2O;   La2O3 vs Sc2O3; Ta2O5 vs Nb2O5 and HfO2¬ vs ZrO2 (Fig. 7) is showed similar variations. Only La2O3 vs Y2O3 shows negative correlation since Y2O3 is much abounded and heavier than La2O3.

**Table5.** Wet-gravimetric analyses of apatite from phoscorite, of Sevvattur

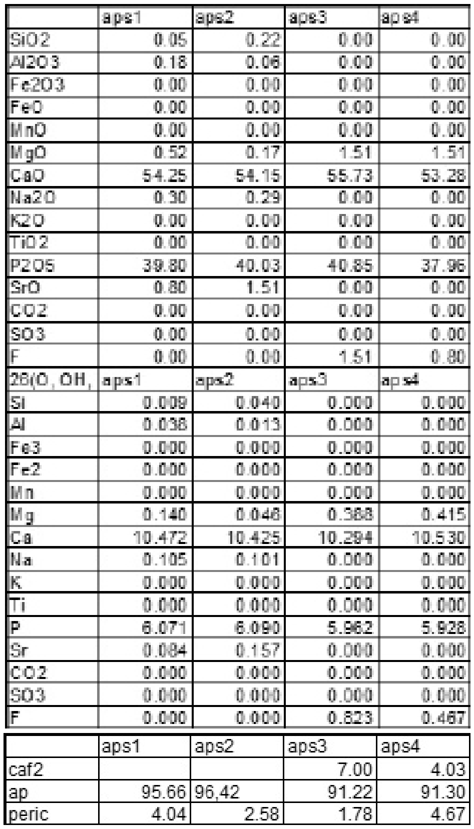

| | aps1 | aps2 | aps3 | aps4 |
|---|---|---|---|---|
| SiO2 | 0.05 | 0.22 | 0.00 | 0.00 |
| Al2O3 | 0.18 | 0.06 | 0.00 | 0.00 |
| Fe2O3 | 0.00 | 0.00 | 0.00 | 0.00 |
| FeO | 0.00 | 0.00 | 0.00 | 0.00 |
| MnO | 0.00 | 0.00 | 0.00 | 0.00 |
| MgO | 0.52 | 0.17 | 1.51 | 1.51 |
| CaO | 54.25 | 54.15 | 55.73 | 53.28 |
| Na2O | 0.30 | 0.29 | 0.00 | 0.00 |
| K2O | 0.00 | 0.00 | 0.00 | 0.00 |
| TiO2 | 0.00 | 0.00 | 0.00 | 0.00 |
| P2O5 | 39.80 | 40.03 | 40.85 | 37.96 |
| SrO | 0.80 | 1.51 | 0.00 | 0.00 |
| CO2 | 0.00 | 0.00 | 0.00 | 0.00 |
| SO3 | 0.00 | 0.00 | 0.00 | 0.00 |
| F | 0.00 | 0.00 | 1.51 | 0.80 |
| 26(O, OH, | aps1 | aps2 | aps3 | aps4 |
| Si | 0.009 | 0.040 | 0.000 | 0.000 |
| Al | 0.038 | 0.013 | 0.000 | 0.000 |
| Fe3 | 0.000 | 0.000 | 0.000 | 0.000 |
| Fe2 | 0.000 | 0.000 | 0.000 | 0.000 |
| Mn | 0.000 | 0.000 | 0.000 | 0.000 |
| Mg | 0.140 | 0.046 | 0.388 | 0.415 |
| Ca | 10.472 | 10.425 | 10.294 | 10.530 |
| Na | 0.105 | 0.101 | 0.000 | 0.000 |
| K | 0.000 | 0.000 | 0.000 | 0.000 |
| Ti | 0.000 | 0.000 | 0.000 | 0.000 |
| P | 6.071 | 6.090 | 5.962 | 5.928 |
| Sr | 0.084 | 0.157 | 0.000 | 0.000 |
| CO2 | 0.000 | 0.000 | 0.000 | 0.000 |
| SO3 | 0.000 | 0.000 | 0.000 | 0.000 |
| F | 0.000 | 0.000 | 0.823 | 0.467 |

| | aps1 | aps2 | aps3 | aps4 |
|---|---|---|---|---|
| caf2 | | | 7.00 | 4.03 |
| ap | 95.66 | 96,42 | 91.22 | 91.30 |
| peric | 4.04 | 2.58 | 1.78 | 4.67 |

Increase of pressure with increasing temperature to the extent of a given density of 8.8 g/cm3 at CMB sudden cracking and creeping develops at lower mantle. Volatiles fill voids initiate widening with developments supercritical fluids. Such supercritical plasmatic bubbles inflate and weaken creeps reduces static friction across their walls. Continental rifting leads direct eruption of natrocarbonatitic supercritical fluids from mantle. These fluids are caused cracking and creeping at mantle for direct effusion of supercritical natrocarbonatitic fluid [32-36]. The Eastern Ghats Paleo Rift system is a continental rift zone [32-35] along which several carbonatites are emplaced in India.

**Table6.** Wet-gravimetric analyses of Phoscorite from Sevvattur Phoscorite from carbonatite of Sevvattur

|  | p1 | p2 | p3 | p4 |
|---|---|---|---|---|
| SiO2 | 16.58 | 9.72 | 3.78 | 16.80 |
| Al2O3 | 5.40 | 2.62 | 0.74 | 5.01 |
| Fe2O3 | 0.00 | 0.00 | 0.00 | 0.00 |
| FeO | 2.73 | 2.98 | 4.68 | 7.08 |
| MnO | 0.00 | 0.00 | 0.00 | 0.00 |
| MgO | 1.46 | 2.36 | 0.98 | 5.16 |
| CaO | 45.37 | 58.16 | 60.10 | 54.52 |
| Na2O | 1.18 | 1.01 | 0.58 | 0.68 |
| K2O | 0.87 | 0.36 | 0.00 | 0.71 |
| TiO2 | 0.00 | 0.00 | 0.00 | 0.00 |
| Nb2O5 | 0.00 | 0.00 | 0.00 | 0.00 |
| P2O5 | 26.42 | 21.35 | 29.13 | 8.80 |
| CO2 | 0.00 | 1.44 | 0.00 | 1.24 |
| Total | 100.00 | 100.00 | 100.00 | 100.00 |
| Rittmann's norm |  |  |  |  |
| ap | 58.59 | 46.55 | 65.81 | 18.74 |
| cc | 0.00 | 3.82 |  | 3.17 |
| mt | 0.41 | 0.46 | 0.78 | 1.13 |
| ol | 20.35 | 19.28 | 7.45 | 30.97 |
| port |  | 21.31 | 23.26 | 31.03 |
| or | 5.60 |  |  |  |
| ab | 2.48 |  |  |  |
| an | 7.26 | 1.45 |  | 8.66 |
| ne | 5.31 | 5.73 | 2.70 | 3.74 |
| ks |  | 1.39 |  | 2.55 |
|  | 100 | 100 | 100 | 100 |

Apatite in carbonatite show rarely primary fluid inclusion carrying ore surrounded by liquid CO2, CO2, brine solutions and water vapour with decrepitating temperature of 750oK. Triple phase inclusions are seen inclusions carrying gypsum brine and water vapour and similar phases occur for halide and sylvite [36]. HPTM appears to be enclosed more than 4 layers of supercritical fluids of natrocarbonatite at mantle horizon. These volatile constituents are associated with alkalis. Globular primary melt inclusions of calcite in clinopyroxene in peridotite and in feldspar in ultrapotassic syenite indicate liquid immiscible separation of carbonatite magma from silicate magma at ambient temperature and pressure at hydrous condition [4].

**Table7.** EDAX analyses of Phoscorite from Onnakarai.

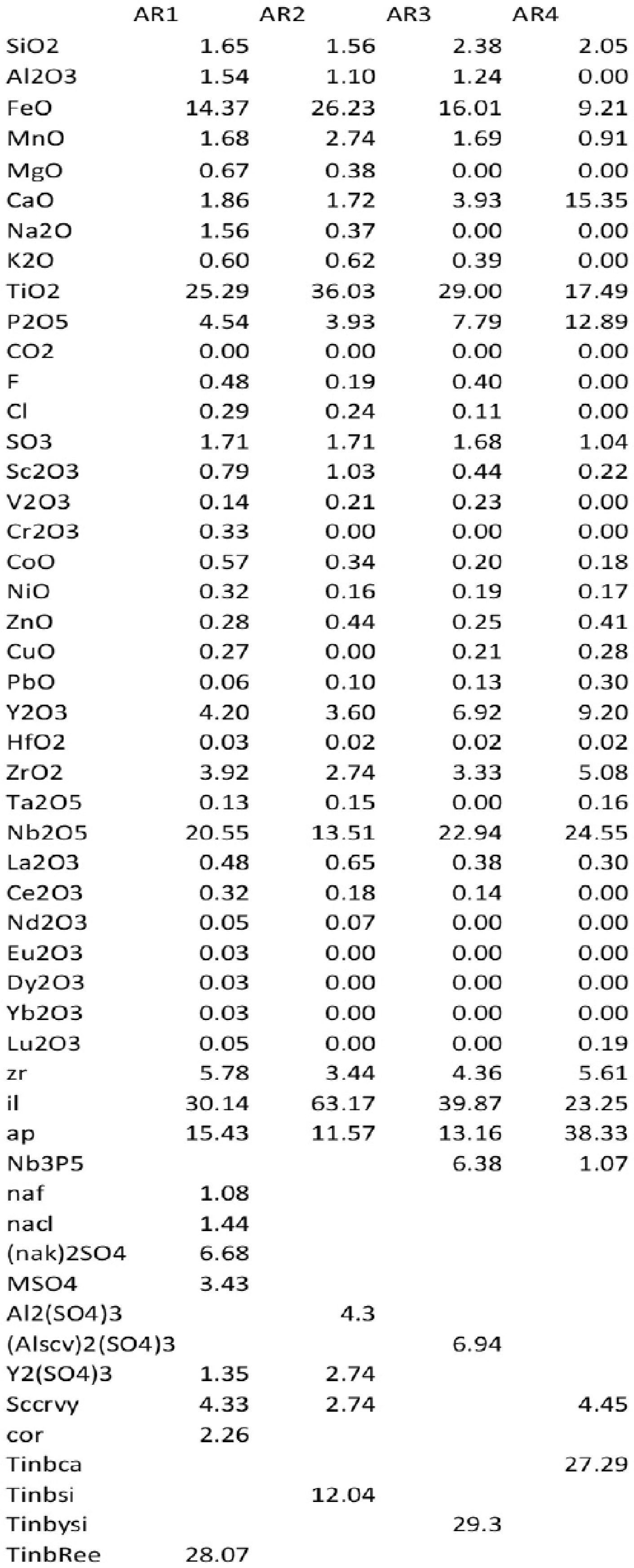

| | AR1 | AR2 | AR3 | AR4 |
|---|---|---|---|---|
| SiO2 | 1.65 | 1.56 | 2.38 | 2.05 |
| Al2O3 | 1.54 | 1.10 | 1.24 | 0.00 |
| FeO | 14.37 | 26.23 | 16.01 | 9.21 |
| MnO | 1.68 | 2.74 | 1.69 | 0.91 |
| MgO | 0.67 | 0.38 | 0.00 | 0.00 |
| CaO | 1.86 | 1.72 | 3.93 | 15.35 |
| Na2O | 1.56 | 0.37 | 0.00 | 0.00 |
| K2O | 0.60 | 0.62 | 0.39 | 0.00 |
| TiO2 | 25.29 | 36.03 | 29.00 | 17.49 |
| P2O5 | 4.54 | 3.93 | 7.79 | 12.89 |
| CO2 | 0.00 | 0.00 | 0.00 | 0.00 |
| F | 0.48 | 0.19 | 0.40 | 0.00 |
| Cl | 0.29 | 0.24 | 0.11 | 0.00 |
| SO3 | 1.71 | 1.71 | 1.68 | 1.04 |
| Sc2O3 | 0.79 | 1.03 | 0.44 | 0.22 |
| V2O3 | 0.14 | 0.21 | 0.23 | 0.00 |
| Cr2O3 | 0.33 | 0.00 | 0.00 | 0.00 |
| CoO | 0.57 | 0.34 | 0.20 | 0.18 |
| NiO | 0.32 | 0.16 | 0.19 | 0.17 |
| ZnO | 0.28 | 0.44 | 0.25 | 0.41 |
| CuO | 0.27 | 0.00 | 0.21 | 0.28 |
| PbO | 0.06 | 0.10 | 0.13 | 0.30 |
| Y2O3 | 4.20 | 3.60 | 6.92 | 9.20 |
| HfO2 | 0.03 | 0.02 | 0.02 | 0.02 |
| ZrO2 | 3.92 | 2.74 | 3.33 | 5.08 |
| Ta2O5 | 0.13 | 0.15 | 0.00 | 0.16 |
| Nb2O5 | 20.55 | 13.51 | 22.94 | 24.55 |
| La2O3 | 0.48 | 0.65 | 0.38 | 0.30 |
| Ce2O3 | 0.32 | 0.18 | 0.14 | 0.00 |
| Nd2O3 | 0.05 | 0.07 | 0.00 | 0.00 |
| Eu2O3 | 0.03 | 0.00 | 0.00 | 0.00 |
| Dy2O3 | 0.03 | 0.00 | 0.00 | 0.00 |
| Yb2O3 | 0.03 | 0.00 | 0.00 | 0.00 |
| Lu2O3 | 0.05 | 0.00 | 0.00 | 0.19 |
| zr | 5.78 | 3.44 | 4.36 | 5.61 |
| il | 30.14 | 63.17 | 39.87 | 23.25 |
| ap | 15.43 | 11.57 | 13.16 | 38.33 |
| Nb3P5 | | | 6.38 | 1.07 |
| naf | 1.08 | | | |
| nacl | 1.44 | | | |
| (nak)2SO4 | 6.68 | | | |
| MSO4 | 3.43 | | | |
| Al2(SO4)3 | | 4.3 | | |
| (Alscv)2(SO4)3 | | | 6.94 | |
| Y2(SO4)3 | 1.35 | 2.74 | | |
| Sccrvy | 4.33 | 2.74 | | 4.45 |
| cor | 2.26 | | | |
| Tinbca | | | | 27.29 |
| Tinbsi | | 12.04 | | |
| Tinbysi | | | 29.3 | |
| TinbRee | 28.07 | | | |

The southern part of Tamil Nadu, a number of carbonatitic lava exposures are seen with air fall tephra, lava flows, tuff, lapilli, pisolites and ashes [41-44].

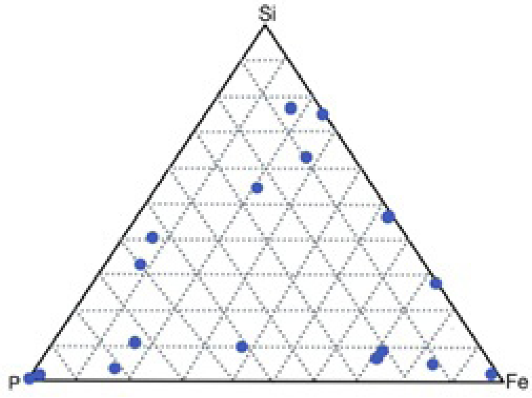

**Fig4.** Distributions of Si, P and Fe+Mn are seen in equilateral triangle. It includes magnetite 5, apatite 5 and phoscorite 9 and a peridotite 1.

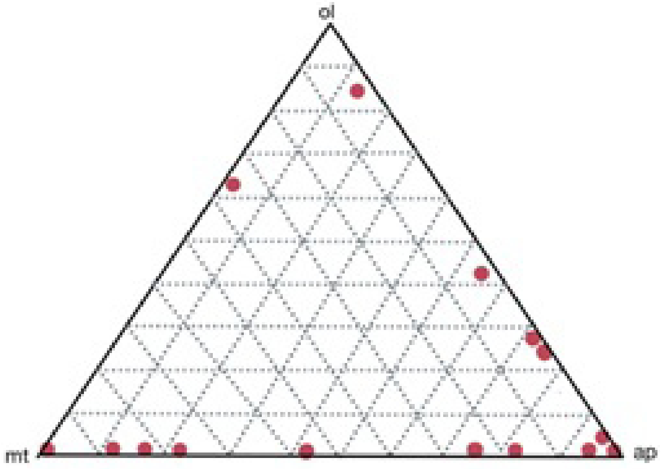

**Fig5.** Distribution of ol, mt, and ap is shown but ol is not included with its heteromorphic variants.

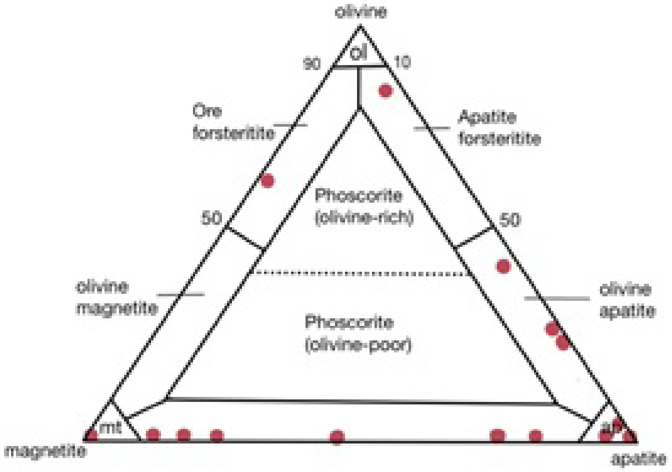

**Fig6.** Classification of Phoscorite is shown. Heteromorphic components of olivine are not included with olivine, If they were olivine rich or poor phoscorite are identified.

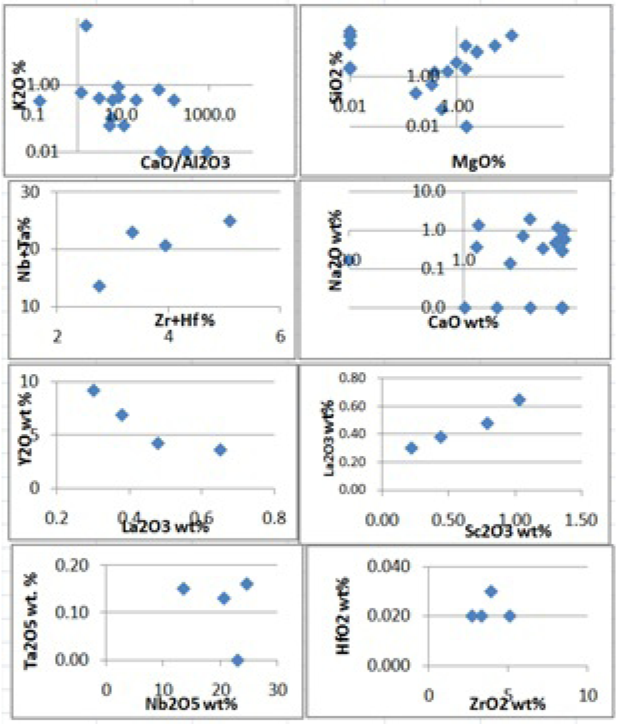

**Fig7.** Bi-component variations of some characteristic chemical components are shown.

## DISCUSION

The petrogenesis of carbonatites and phoscorites at mantle source remain as an unsolved problem. The cause ultralow velocity seismic zone is detected near core - mantle boundary (CMB) is not clearly known [27,]. Recent discovery of presence of primary natrocarbonatite melt inclusions in diamond from mantle source has revised origin of supercritical natrocarbonatite. Occurrence of sodium fluorite, sodium chloride and sodium potassium sulphate (Table 7) indicates that the primary fluid is natrocarbonatite from lowermost mantle. SO3 is present in syenites and ultramafic rocks up to 1.75 wt%., in this complex. HPTM [28, 29] inclusions enclosed by multiple layers of fluids to maintain its stability. A large quantity of potential/latent energy is consumed or released for the formation / deformation of layers enclosed or around HPTM as that of homogenization in fluid inclusion of multiple phases. Such behaviour preserves the stability of ascend of HPTM. During course of magmatic differentiation volatiles and alkalis are concentrated in the residual magma. The released H2O, C, O, F, S, P silica and alkalis are consumed by younger crystallizing minerals under alternate miaskitic and agpaitic environment [18, 20, 21].

Studying C-O-H system CH4, C2H6 and other hydrocarbons are possible to generate under HPT conditions [31] at deep mantle. These hydrocarbons and H2, He, H2O, N, CF4, C4F8 and SF6 exist as supercritical fluids above their critical temperatures of 300°C in wide range of pressure conditions from 300 MPa to 300 GPa [32]. Solvent power of supercritical fluid of CH4 and H2O increases at this state.

The discovery of natrocarbonatite inclusions in diamond [28-30] is illustrated by presence of ultralow viscous supercritical natrocarbonatite fluid in lowermost mantle near CMB. Small degree of partial melting of dense carbonated peridotite releases [38] primary natrocarbonatite fluids energized with enrichment of elements of low atomic numbers of H, He, C, O, F, Na, Mg, Al, Si, P, S, Cl. K, Ca, Sc, Ba, Ti, Mn. LREE and Fe at HPT state excerpts pressure inducing creeping and cracking. Through such conduit supercritical fluids of natrocarbonatite carrying HPTM enveloped by multi-layered fluids ascends at a speed of from 70 to 100 m/s within 10 hours duration to Earth's surface retains its structural stability [30, 45, 46]. There is not enough time for structural change.

## CONCLUSION

The carbonatite complex of Tiruppattur is unique of its differentiated and fractionated co-magmatic sequences of alkaline and carbonatite rocks [1-6]. The ultralow viscous supercritical natrocarbonatite fluid at lower mantle may be developed by low degree of partial melting of carbonated peridotite mantle at depth. HPTM of Si-perovskite, Ca-perovskite, zircon, periclase apatite and ilmenorutile are crystallized at its early stage of development of supercritical fluid [40]. Geophysicists believe that mantle horizon near CMB is highly heterogeneous because of development of ultralow velocity zones for seismic waves due to presence of ultralow viscous primary supercritical natrocarbonatite fluid. The supercritical natrocarbonatite fluid carrying HPTM surrounded by HPT layers ascends very rapidly at a speed of 70-100m/s without any friction and loss of potential energy [39, 45, 46] through suddenly developed creep / conduit in lower mantle. HPTM does not any structural change near surface. The natrocarbonatite fluid is the parent magma for differentiated phoscorite in this carbonatite complex of Tiruppattur.

## ACKNOWLEDGEMENT

The author expresses his sincere thanks for the staff of (1977-80) Geochemical Laboratory and Department of Crystallography Moscow State University, Russia. He thanks for co-operation of Thiru. T. Ragavaiyya during EDAX analyses of phoscorite in the Department of Material Sciences and Metallurgical Engineering, Indian Institute of Technology, IITM, Chennai, 600 036. Grateful thanks are due to Dr. V. Subramanian Ex. Additional Director, Department of Geology and Mining for his field guidance and moral support. Finally, the author thanks Dr. S. Saravanan and his wife Mrs Kasthuri Saravanan who maintained perfect Guru-Shisya Parmpariya throughout the entire research period between July1967 and July 1973 in Presidency College, Chennai.

## REFERENCES

1. R, Ramasamy, Geology of the area South west of Tiruppattur, Madras State (Tamil Nadu), India, Ph.D. Thesis, pp226, University of Madras, July, 1973.
2. R. Ramasamy, Structure and tectonics of carbonatite complex of Tiruppattur, Tamil Nadu In: Bhattacharya, A..K. (Edr.) Current Trends in Geology, IV Indian Geological Congress, Today and Tomorrows Publishers, New Delhi, pp. 119-136, 1982.
3. S. Saravanan and R. Ramasamy, A magnesioriebeckite from Samalpatti area, Tamil Nadu, India, Mineralogical Magazine, 38, 376-377, 1971.
4. S. Saravanan and R. Ramasamy, Geochemistry and petrogenesis of shonkinite and associated alkaline rocks of Tiruppattur carbonatite complex, Tamil Nadu, Journal of the Geological Society of India, 46, 235-243, 1995.
5. R. Ramasamy, Crystallization, fractionation and solidification of co-magmatic alkaline series sequentially emplaced in carbonatite complex of Tiruppattur, Tamil Nadu, India, Book on Crystallization- Science and Technology, Edrs Marcello Rubens, Barsi Andreeta, ISBN, 535- 564, 12th Sept. 2012, INTECH, Austria.
6. R. Ramasamy, P. S. Dhote, S. F. R. Kadri, and L. G, Gwalani, Carbonatite alkali complex of Tiruppattur South India: 1 Petrography and Petrochemistry of the carbonatites, Indian Journal of Geochemistry,19, 167-187. 2004.
7. R. Ramasamy, Ultrabasic nodules in skarn rocks of Garigaipalli, Group Discussion –Carbonatites- Journal of Geol. Soc. India, Bangalore p. 5, 1976.
8. R. Ramasamy, S. P. Subramanium and R, Sundaravadivelu, Mineralization of Galena in an aplitic albitite from carbonatite complex of Tiruppattur, Tamil Nadu, India, IOSR – IAGG, 1, (3) Sept-Oct, 54-65, 2013.
9. R. Ramasamy, Ultrapotassic rocks from carbonatite complex of Tiruppattur, Tamil Nadu, IJISSET, 6 (7) 48-54, 2020
10. J.C. Grady, Deep main faults in South India, Journal of the Geological Society of India, 12, 56-62, 1971.
11. A. Rittmann Stable Mineral Assemblages of igneous Rocks, Springer-Verlag, Berlin, 264p, 1973.
12. R. Ramasamy, L.G. Gwalani, and S.P. Subramanian, A note on the occurrence and formation of magnetite in the carbonatites of Sevvattur, North Arcot district, Tamil Nadu, Southern India Journal of Asian Earth Sciences, 19, 297-304, 2001
13. W,A, Deer, R, A, Howie and J. H. Zussman, An Introduction to the Rock Forming Minerals, Pearson Prentice Hall, London, 696p 1992
14. A. Taufiq, A. Nikma, A. Hidayat, S. Sunryona, N. Mufti, N. Hidayat, H. Susanto Synthesis of magnetite / silica particle

composites from natural sand to create drug delivery vehicle, Helion, 6 (4)1-10 2020

15. R. Ramasamy, Ca-rich pyroxenes from carbonatite complex of Tiruppattur, Current Science, 55 981-984, 1986.
16. R. Ramasamy, Titanium bearing garnets from alkaline rocks of carbonatite complex of Tiruppattur, Tamil Nadu, Current Science, 55 1026-29, 1986.
17. T, H Green and E.B, Watson, Crystallization of apatite in natural magmas at high pressure, hydrous conditions with particular references to Orogenic tock series, Contrib. Mineralogy and Petrology, 79 96-105, 1982.
18. R, Ramasamy, Mineralization of nioborutile, hercynite and other iron oxide minerals on ultramafic body in the carbonatite complex of Tiruppattur, Tamil Nadu, IJISSET, 4 (6), p. 12-18, 2018.
19. R. Ramasamy, Ultramafic rock of carbonatite complex of Tiruppattur, India, IJISSET, 4 (12), 16-22. 2018.
20. K. Yagi, Petrochemical studies on the alkaline rocks of the Morotu District, Sakhalin, GSA Bull, v. 64, 769-810, 1953.
21. N. L. Bowen, The Evolution of Igneous Rocks, Dover, New York, 2nd Edn 332p 1956.
22. E. Wm. Heinrich, Microscopic Petrography, Mc Grew Hill, New York, viii+296, 1956
23. M. J. Le Bas, Nephelinites and carbonatites, Geol. Soc. London Spl. Pubn 30, 53-83, 1st Jan, 1987.
24. H. Downes, E. Balaganskaya, A. Beard, R. Liferovich, D. Demaiffe, 2005: Petrogenetic processes in the ultramafic, alkaline and carbonatitic magmatism in the Kola Alkaline Province: a review. Lithos 85, 48–75.
25. E. G. Balaganskaya, H. Downes, D. Demaoffe, REE and Sr-Nd isotope compositions of clinopyroxenites, phoscorites and carbonatites of the Seblyavr massif, Kola Peninsula, Russia, Mineralogia, Polonica, 38 (1) 1-17, 2007.
26. L. L. Panina, I. V. Motorina, Liquid immiscibility in deep-seated magmas and the generation of carbonatite melts. Geochem. Int. 46, 448–464 2008.
27. Nataly Krosnova, Introduction to phoscorites, occurrence, composition, nomenclature, and petrogenesis In book phoscorites and carbonatites from mantle to mine: the key example of the Kola Alkaline Province, edrs. A. Zaitsev and F, Wall, Mineralogical Society series, (10), Chapter 2, p. 44-72, 2004
28. J. F. Justo, and D. A. Yuen, Viscosity undulations in the lower mantle : the dynamical role iron spin transition, Earth and Plnetary Science Letters, 421, pp. 20-26, 1st July, 2015.
29. F. V. Kaminsky, T. Wirth, A. Schreiber, Carbonatitic inclusions in deep mantle diamond from Junia Brazil : New minerals in the carbonate-halide association, The Canadian Mineralogist,51 (5), 669-688, 2013
30. F. V. Kamindky, I. D. Ryabchiokov and R. Wirth, A primary natrocarbonatite association in the Deep Earth, Mineralogy and Petrology, 110, 387-398, 2016,
31. Chi Zhang and Zhenhao. Duan Zhang. A model for C-O-H fluid in the Earth's Mantle ScienceDirect, 73, (7) 2089-2102 1St April 2009
32. Ramachandran Ramasamy, Subramanum Subramanium and Ranganathan Sundaravadivelu., Formation of Gas hydrates at deep interior of the Earth and their dissipation to near surface horizon, Journal of Geological Research, 2013, 1-11 ID 207031 10th Dec. 2013.
33. R. Ramasamy, A possible paleo-rift system of the Eastern Ghats in Peninsular India, J. Moscow State Univ., Geology, Ser 4(2),pp 32-37 (Russian) 1982
34. R. Ramasamy, Reactivation of the Eastern Ghats Paleorift system during Tertiary and other periods, Proc. National, Seminar Tertiary Orogeny, BHU, Varanasi,. 109-127. 1987.
35. D.K. Bailey, Volatiles in alkaline magmatism, Lithos, 26 (1-2) 157-165, 1990 Continental rifting and mantle degassing, E.R. Neumann I.B. Ramberg (Edr.)
36. D.K. Bailey, Mantle carbonatite eruptions, Crustal context and implications, Lithos, 26, (9), 37-42, 1990.
37. R. Ramasamy, and V, Shapenko, Fluid inclusion studies in carbonatites of Tiruppattur, Tamil Nadu, India (Abst.) Int. Geol. Cong. Paris, v. 1, p. 79, 1980.

38. Yanhao Lin, Quing Yang Hu, Li Zhu and Yue Meng, Pressure Temperature implication for a New Reservoir of flour in the Deep Earth, Minerals, 10, p. 783, 2020.
39. Leduc Ludovic, Lucia Gurioli, Andrew Harris, Livio Colo and Estelle Tose-Koga, Types and mechanisms of Stombolian explosions, Characteristion of gas dominated explosion at Stomboli, Bulletin of Volcanology, 77 (8) 1-15. 24th January, 2015.
40. F, Nestola, N. Korolev,M. Kopylova, N. Rotiroti, D, G, Pearson, D. G. M.G. Pamato, M, Alvaro, L Peruzzo, J. J, GurneyA, E. Moore, J. Davidson, CaSiO3 perovskite in diamond indicates the recycling of oceanic crust into the lower mantle, Nature. 555 (7695): 237–241 (March 2018).
41. R, Ramasamy, Carbonatite bombs, lapillus, pisolites and ashes in semi unconsolidated gritty conglomerate of Early Pleistocene, from Thiruvalangadu, Tamil Nadu, India, Int. Journal, Engineering and Applications, 4 (8) 112-119, 2014.
42. R, Ramasamy Geochemical studies on carbonatite lava flows occurring in and around Kudangulam area, Tamil Nadu, India, IJISSET, 2017, 3 (9) 23-30.
43. R. Ramasamy, Carbonatite-tuff in Sattangulam and other parts of Tamil Nadu, IJISSET, 5. (9), 28-32, 2019.
44. R. Ramasamy, Geochemistry of Fumarolic deposition of carbonatite volcanism in Tamil Nadu. IJISSET, 6 (9) 4-12, 2020.
45. N. E. Timms, et.al, A pressure, temperature phase diagram for zircon at extreme conditions, Earth Science Reviews, 165, 185-202, 2017
46. R. Ramasamy, Silicate-perovskite (Si-Fe-Nb-Ca-Ti) lava flows in Tamil Nadu, IJISSET 2 (11) Nov. pp. 8-15. 2016.

AUTHORS' BIOGRAPHIES

Dr. R. Ramasamy, M.Sc, Ph.D 1974 and P.D.F. (MSU 1977-80), was a Petrologist in Dept. of Geology & Mining. Proj. Advisor, C.E & OE, IITM.

**Citation:** *R. Ramasamy. Michael Terfa Angura. Phoscorite From Ultrabasic Rock in Carbonatite Complex of Tiruppattur, Tamil Nadu, India. Int J of Innovative Studies in Sciences and Engineering Technology. 2021; 7(1): 11-24. DOI: https://doi.org/10.20431/2455-4863.070102.*